THE IMPROVEMENT OF DOWNCOMER AND LOWER-PLENUM MODEL OF CHINSHAN NUCLEAR POWER PLANT BY USING CFD SIMULATION

Yu-Ting Ku, Yung-Shin Tseng

Department of Engineering and System Science, National Tsing Hua University

No. 101, Section 2, Kuang-Fu Rd., Hsinchu, Taiwan, R.O.C.

Shao-Wen Chen

Institute of Nuclear Engineering and Science, National Tsing Hua University

No. 101, Section 2, Kuang-Fu Rd., Hsinchu, Taiwan, R.O.C.

Jong-Rong Wang, Chunkuan Shin, Yum-Fei Chang

Nuclear and New Energy Education and Research Foundation

No. 101, Section 2, Kuang-Fu Rd., Hsinchu, Taiwan, R.O.C.

ABSTRACT

In the past study, a commercial CFD model was established to investigate thermal-hydraulic phenomena in downcomer and lower-plenum of boiling water reactors (BWRs), and the analyses of the CFD model under steady operations as well as transient status were completed by using CFD code, FLUENT. Owing to model simplification, flow resistance caused by ignored components, such as fuel assembly, separator, and steam dryer, was not considered. However, the flow resistance has certain effects on follow-up calculations on flow velocity and pressure field. As a result, the reliability of the simplified model decreased. This study focused on the improvement of the vessel model with considering the flow resistance caused by ignored components in the previous research, and the effects of the flow resistance was represented via an added porous zone at the outlet of the simplified model. The porous zone was generated to reach the purpose of approaching actual flow field and pressure distribution under operating conditions. The results showed that the pressure distribution and the flow field at the core inlet region were more approaching to the actual status in the improved model. We expected the results of the steady state of the improved model could be utilized on the initialization of transient events, and facilitated the safety analysis under different transient events afterwards.

1. Introduction

With the rising and continuous concerns about nuclear operating systems and nuclear safety issues, nuclear safety analysis has become one of the main research subjects on nuclear development. Therefore, many experimental and simulation results have been proposed to enhance the reliability of nuclear safety research. In order to improve the accuracy of the nuclear safety analysis, various codes have been

developed, such as TRACE [1], RETRAN [2], and FRAPCON [3]. Those system codes can only be calculated in one dimension only with simplified three-dimensional vessel models. However, the local characteristics and effects cannot be presented in three-dimensional space by using the codes mentioned above. This is significant to crucial components in complicated transient states or accidents.

In a decade, commercial Computational Fluid Dynamics (CFD) codes were introduced as a nuclear safety analysis tool, and the ability of calculating the thermal-hydraulic distribution in three-dimensional complex geometry model was extraordinary. This was shown by the simulation outcomes which were generally similar to experimental data. As to the crucial components, such as reactor pressure vessel, building up a three-dimensional model with proper boundary conditions by CFD codes was more efficient and cost-saving than experiments. This would be the advantages of using CFD codes in the safety analysis of nuclear power plants (NPPs).

In the previous study [4], a CFD model was generated for investigating thermal-hydraulic behaviors and mixing phenomena in the downcomer and the lower-plenum of the Chinshan nuclear power plant (CSNPP). Moreover, the inadvertent start of High Pressure Coolant Injection (HPCI) event was analyzed by the CFD model, and the results of HPCI event were further provided to RETRAN in order to revise thermal-hydraulic parameters of RETRAN. Owing to model simplification, flow resistance caused by ignored components, such as fuel assembly, separator, and steam dryer, was not considered. However, the flow resistance has certain effects on follow-up calculations on flow velocity and pressure field. As a result, the reliability of the simplified model decreased.

The object of this study focused on the improvement of the vessel model with considering the flow resistance caused by ignored components in the previous research, and the effects of the flow resistance was represented via an added porous zone at the outlet of the simplified model. The porous zone was generated to reach the purpose of approaching actual flow field and pressure distribution under operating conditions.

2. Geometrical model and mesh generation

In this paper, the model was generated based on the previous one with an newly added porous zone to represent the flow resistance of ignored components. The porous zone was located at the outlet of the simplified model in order to revise the pressure field of the entire model. It could further prevent follow-up miscalculation caused by the result of the wrong pressure field so as to maintain the reliability of the model at a good level.

The flow chat of simulation was showed in Fig. 1. In the reality, the vessel is divided into four regions, downcomer, lower-plenum, core, and upper-plenum region. In the previous model, only the downcomer and the lower-plenum were structured and totally ignored the other two regions in the vessel. In this research, a porous zone were created to present the ignored regions, which were the upper-plenum and the core. The purpose of a newly added porous zone in the three-dimensional vessel model of the Chinshan plant was to present the thermal-hydraulic behavior.

In this model, the downcomer was composed of feedwater lines, feedwater sparger ring, spargers, jet-pumps and recirculation loops (RECIRCs). In addition to the

downcomer, control rod guide tubes, core support, peripheral and orificed fuel supports were structured in the lower-plenum (of the model). Moreover, components in the core and the upper-plenum, such as fuel assembly, separator, and steam dryer, were simplified as a porous zone. The entire model was showed in Fig. 2.

A commercial CFD code, FLUENT [5], was used for this calculation. For calculating time savings and convergence, assumptions and simplifications in the model were described as follow:
1. Since the saturated water from the separator was a constant flow with a steady temperature under the normal operation, the detailed geometry of the separator was simplified as a free surface with inlet boundary conditions of saturated water.
2. RECIRC piping systems and the inlet manifold of jet-pumps were ignored for reducing the difficulty of modeling. An extra user defined function (UDF) [6] was utilized to simulate the corresponding flow rates and average temperatures between the RECIRC suction, the inlet manifold of jet-pumps and jet-pump injection. The results of UDF calculation was utilized as a uniform distribution at jet-pump outlet.
3. The core and the upper-plenum were ignored, but the flow resistance was considered by adding a porous zone in order to approach actual flow field and pressure distribution under operating conditions.

An unstructured mesh system was employed to generate the meshes in this model (Fig. 3). The total grids were about 12.48 million with tetrahedral/ hexahedral/ wedge meshes, and the maximum mesh skewness was controlled below 0.93.

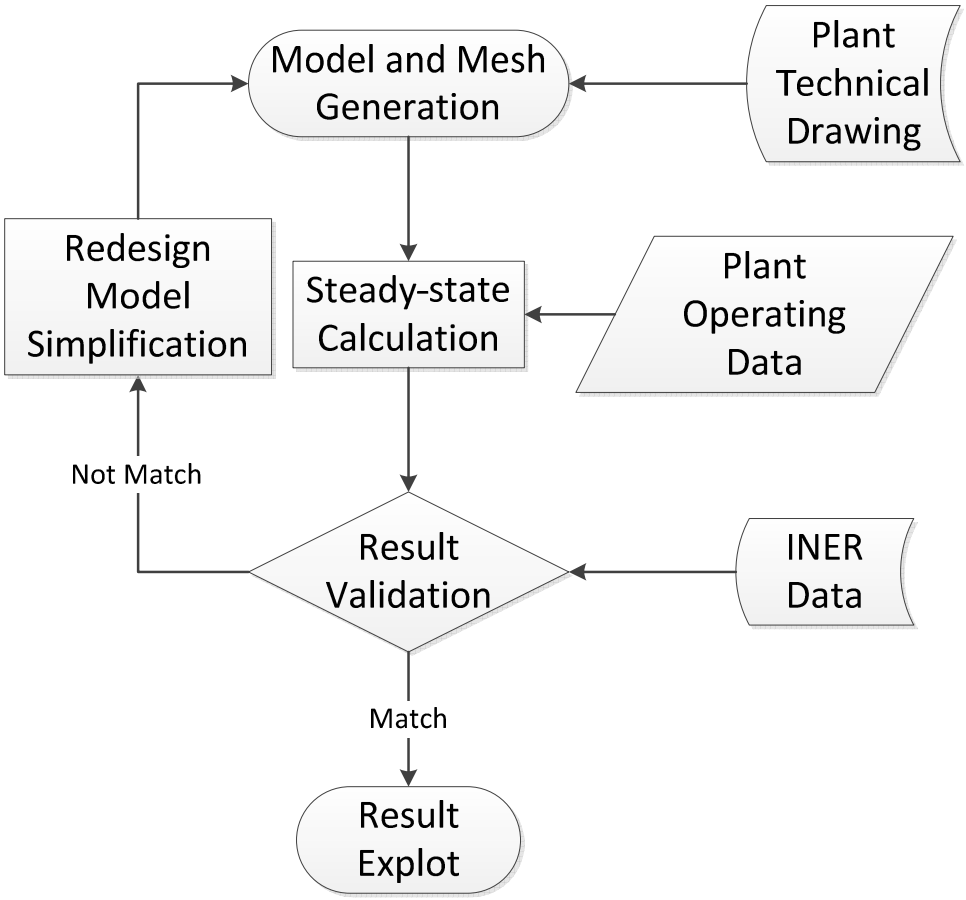

Fig. 1. Flow chat of entire CFD calculation.

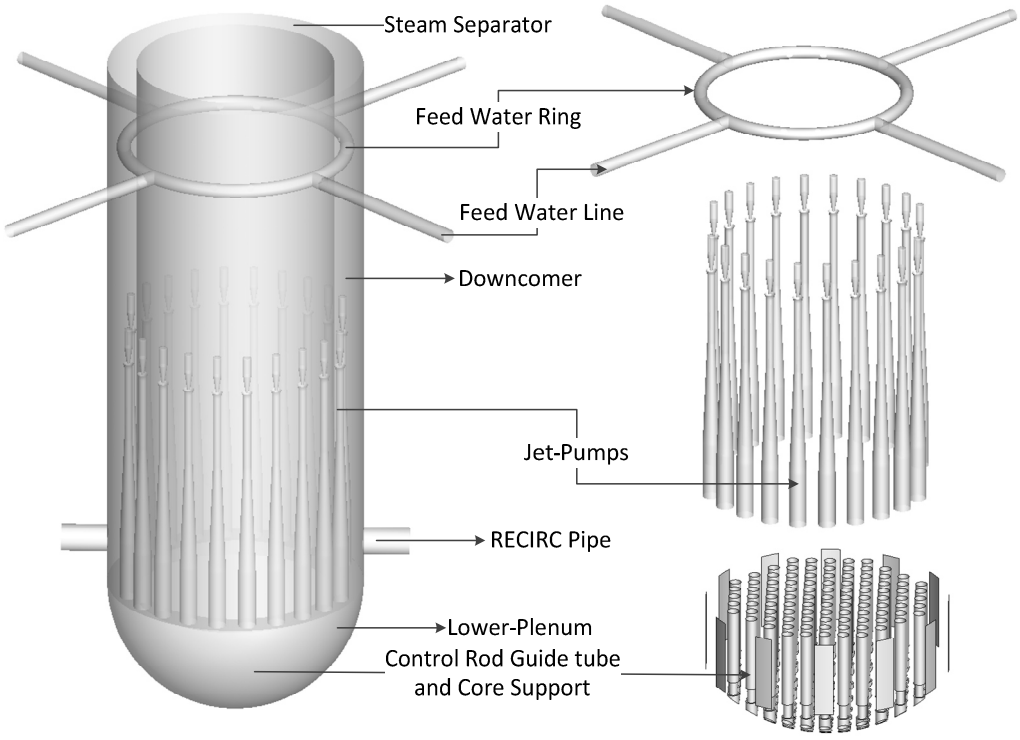

Fig. 2. CSNPP 3D model of CFD simulation.

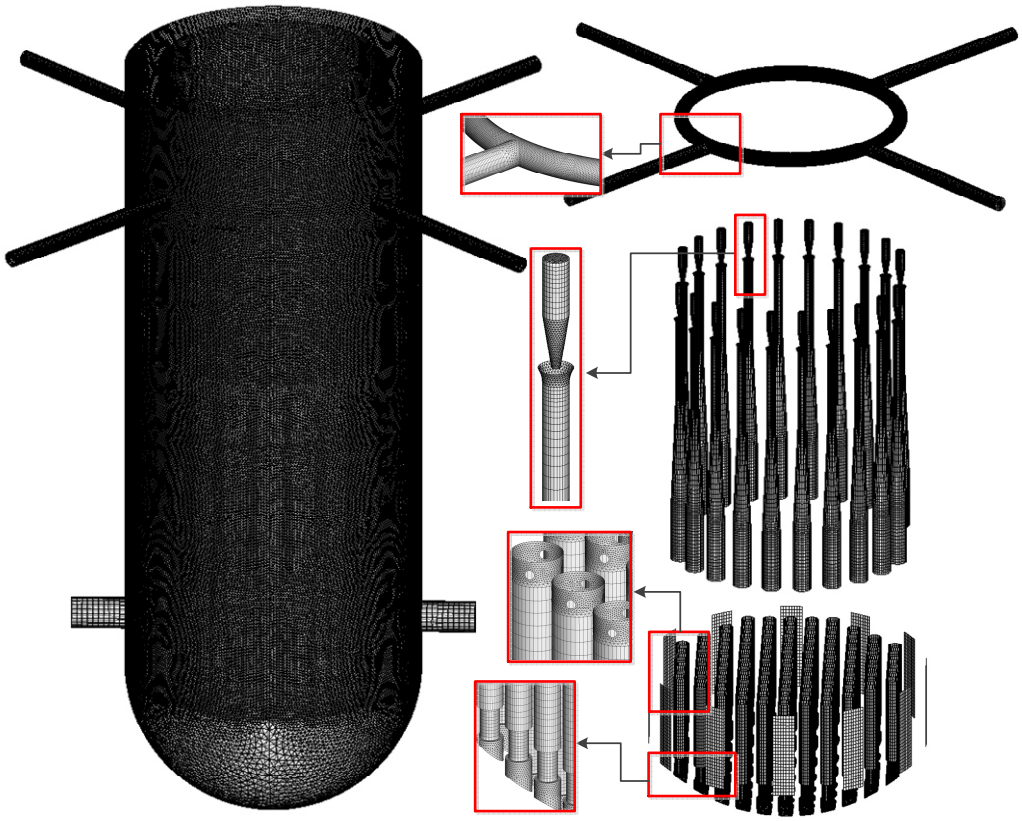

Fig. 3. Mesh distribution of CSNPP 3D model.

3. Mathematical and numerical model

The governing equations for an incompressible and transient problem with no heat source can be written as:

Continuity Equation:

$$\frac{D\rho}{Dt} + \rho \nabla v = 0$$

Momentum Equation:

$$\rho\frac{\partial u}{\partial t} + \rho\left(u\frac{\partial u}{\partial x} + v\frac{\partial u}{\partial y} + w\frac{\partial u}{\partial z}\right) = -\frac{\partial P}{\partial x} + \mu\left(u\frac{\partial^2 u}{\partial x^2} + v\frac{\partial^2 u}{\partial y^2} + w\frac{\partial^2 u}{\partial z^2}\right)$$

$$\rho\frac{\partial v}{\partial t} + \rho\left(u\frac{\partial v}{\partial x} + v\frac{\partial v}{\partial y} + w\frac{\partial v}{\partial z}\right) = -\frac{\partial P}{\partial y} - \rho g + \mu\left(u\frac{\partial^2 v}{\partial x^2} + v\frac{\partial^2 v}{\partial y^2} + w\frac{\partial^2 v}{\partial z^2}\right)$$

$$\rho\frac{\partial w}{\partial t} + \rho\left(u\frac{\partial w}{\partial x} + v\frac{\partial w}{\partial y} + w\frac{\partial w}{\partial z}\right) = -\frac{\partial P}{\partial z} + \mu\left(u\frac{\partial^2 w}{\partial x^2} + v\frac{\partial^2 w}{\partial y^2} + w\frac{\partial^2 w}{\partial z^2}\right)$$

Energy Equation:

$$\frac{\partial T}{\partial t} + \left(u\frac{\partial T}{\partial x} + v\frac{\partial T}{\partial y} + w\frac{\partial T}{\partial z}\right) = -\alpha\left(u\frac{\partial^2 T}{\partial x^2} + v\frac{\partial^2 T}{\partial y^2} + w\frac{\partial^2 T}{\partial z^2}\right)$$

Due to the high velocity and the complex geometry problem, flow patterns and mixing phenomena are significantly associated with the turbulence. Thus choosing an appropriate turbulence model by comparing with experiment data would assist us in enhancing the accuracy of flow behavior calculation. Three common turbulence models including RNG *k-ε* model, realizable *k-ε* model and SST *k-ω* model were applied for this problem. The results of three turbulence model were compared with the previous study to assess the performance of the thermal-hydraulic behavior.

4. Boundary condition and simulation method

FLUENT provided several methods to solve the spatial discretization, including First-order upwind scheme, Second-order upwind scheme, Power Law, etc. In this case, Second-order upwind scheme was utilized to solve the governing equations, and the convergent residues for/of energy, momentum and other equations were must less than 10^{-5}, 10^{-3}, and 10^{-3} respectively. In the solution of pressure field, Semi-Implicit Method for Pressure-Linked Equations-Consistent (SIMPLE-C) [7] was selected. The boundary conditions of steady state were followed the previous study and listed in Table 1.

Initial conditions	Values
Feedwater lines	
Mass flow rate (kg/s)	243
Temperature (K)	488
Steam separator	
Mass flow rate (kg/s)	5682
Temperature (K)	560
Driving flow of jet-pump(group)	
Mass flow rate (kg/s)	1920

Temperature (K)	Calculated by UDF
Recirculation loops	
Velocity (m/s)	8.7
Temperature (K)	Calculated by UDF

Table 1. Initial conditions in the analysis of normal designed function.

5. Results and discussion

For demonstrating the difference between diverse methods, the mass flow rate and pressure at core inlet region of different methods were compared in this study. Due to the mass flow rate was one of effective factors of the thermal-hydraulic behavior at core inlet region, and the mass flow rate was depend on the flow area of fuel support. There were two types of fuel supports, the peripheral and orificed fuel supports, at core inlet region. In this study, the pressure and mass flow rate of fuel supports at specific locations were compared with previous research and the RETRAN data from Institute of Nuclear Energy Research (INER).

As shown in Fig. 4, the similar trend was presented at the curves of three turbulence model. Due to the geometry of lower-plenum, there had no core supports to block the working fluid from jet-pump injection at 45 degree, 135 degree, 225 degree, and 315 degree. It caused less secondly flow than other locations at outskirt of core inlet region and made the mass flow rate of peripheral fuel support decreased. Comparing with RETRAN and previous study, the effects from geometry and secondly flow at outskirt of core inlet were more obvious in this improved model. At middle of core inlet region, since the centralized flow direction and the pressure revised from porous zone, the mass flow rate were more stable than other models (Fig. 5).

The pressure value at outskirt of core inlet region with different methods was showed at Fig. 6. The outlet pressure was a constant value, 1044 psi, as a boundary condition in the previous study. In the present model, the pressure was also affected by the geometry of lower-plenum and secondly flow, and the curves were oscillated with a similar trend in three types of turbulence model. The curve of RETRAN model was flattened due to the effect of geometry was not considered in calculation. At middle of core inlet region, the curve of pressure was similar with mass flow rate since the same effects (Fig. 7). In the pressure distribution of middle and outskirt of core inlet region, the slight divergence of result in three different turbulence models was due to the different coefficient relations of turbulence factors and pressure. From the above results, it could be seen that the similarity between RETRAN and CFD results. Then, the hydraulic behavior and mixing phenomenon of the CFD model were discussed.

As shown in Fig. 8, a scattering distribution of flow direction was found at point A since the feedwater was hit the inner wall of feedwater ring, and flow direction was more consistent at far side from feedwater inlet (point B). There was more clearly explained at Fig.9, the cooling water from feedwater line was hit the inner wall of feedwater ring and separated into two directions. At the same time, some of feedwater was flowed out via feedwater nozzles (point A). Since the point A had two flow direction, the radial way was from the feedwater nozzles, and the axial direction was from the hot water of separator. There was better flow mixing due to the flow velocity decrease.

Under the influence of the flow field, the temperature field in the downcomer was also presented a symmetrical phenomenon. The temperature difference was about 65K before the working fluid mixing in the downcomer. There could found an obvious temperature drop locating at outlet of feedwater nozzle when the working fluid were mixed in the downcomer (Fig. 10). The working fluid was evenly mixed in the downcomer, and the temperature difference was below 4K before the fluid was sucked into jet-pumps inlet and RECIRC inlet (Fig. 11).

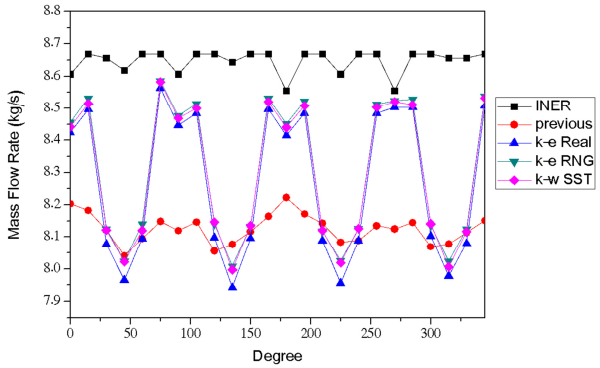

Fig. 4. Mass flow rate of different calculation at outskirt of core inlet region.

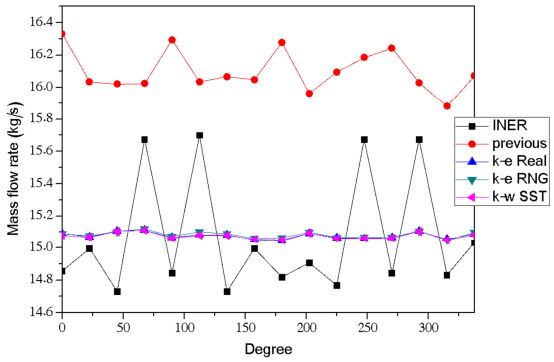

Fig. 5. Mass flow rate of different calculation at middle of core inlet region.

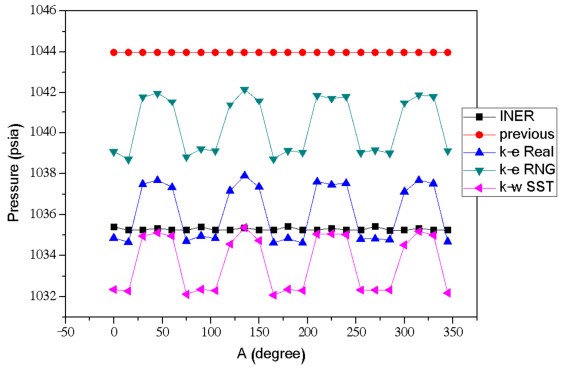

Fig. 6. Pressure field of different calculation at outskirt of core inlet region.

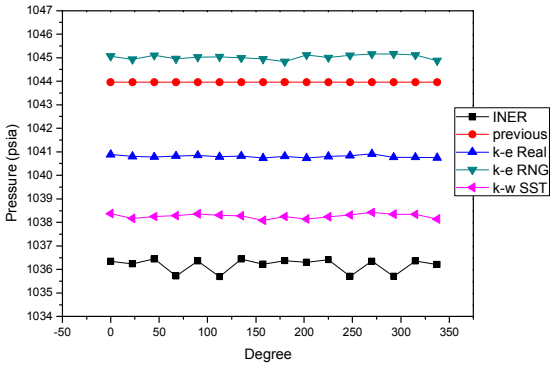

Fig. 7. Pressure field of different calculation at outskirt of core inlet region.

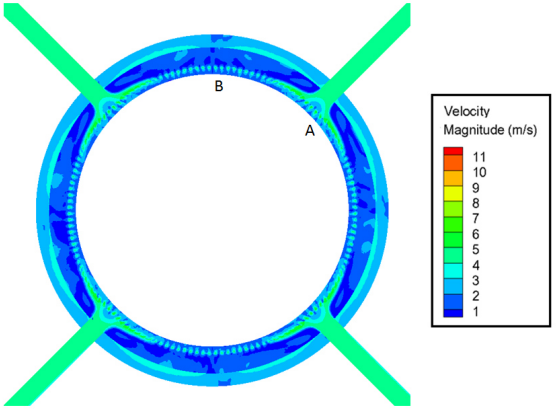

Fig. 8. Velocity distribution of feedwater ring.

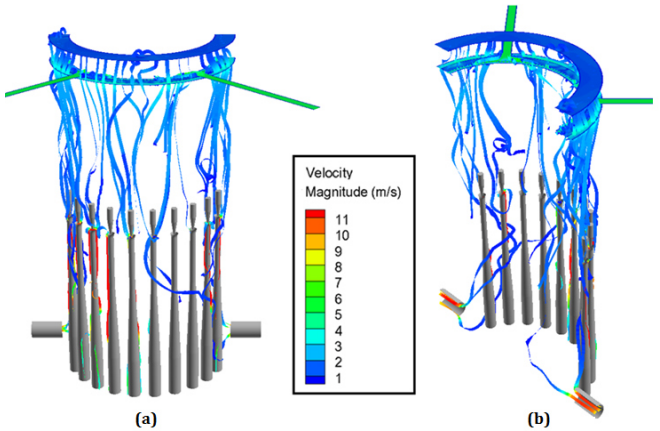

Fig. 9. Streamline in downcomer (a) Front view, (b) Lateral view.

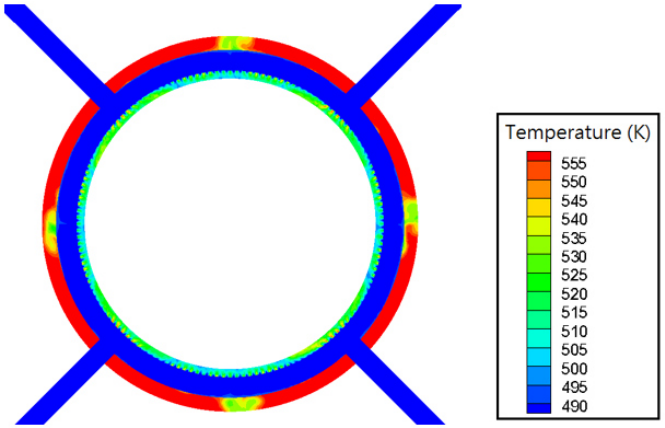

Fig. 10. Temperature distribution of feedwater ring.

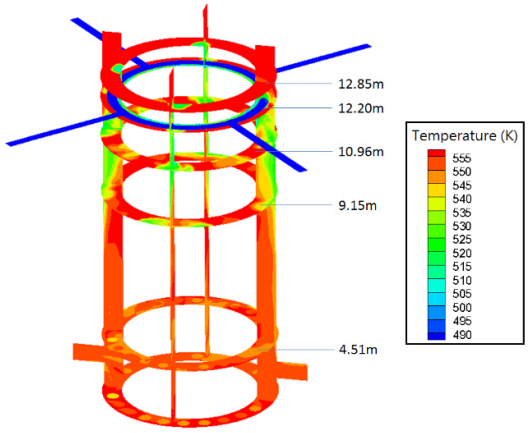

Fig. 11. Temperature distribution of different height in downcomer.

In the lower-plenum, the geometry was the same as the past study, and the results also similar. There was no strong cross flow due to small space with 97 control rod guide tubes. The mixing effect between the injecting water of each jet pump was lightly increase the entire mixing, and most of working fluid was changed flow direction to axial direction due to the bowl shape of lower-plenum. A very similar temperature and velocity distribution along the axial height was presented at Fig. 12 to Fig. 15. Poor mixing in the lower-plenum was confirm.

6. Conclusions

In this study, the CFD model of CSNPP in the past research was improved to investigate the steady analysis. The model results was comparing with RETRAN results, and the CFD result shows that the similar trend was presented at the curves of three turbulence model, but lightly difference with RETRAN curve due to the effect of geometry was not considered in RETRAN calculation.

According to the CFD result, there are several findings, which include:

- Under normal operation, downcomer, annulus region between core shroud and vessel wall, is the major mixing region, and it is limit for the cold supplement water and the saturated one.
- Jet-pumps supply to harmonize the driving and suction flow to a uniform temperature, and the mixing flow discharges to the lower-plenum through the diffuser.
- Due to the small gap and high velocity, poor mixing is existed in lower-plenum.

This study successfully established a CFD model for Chinshan BWR pressure vessel, and the analysis of normal operation had been identified. It could be expected that transient event was analyzed through this model. Furthermore, the analysis result could be provided for system/neutronic codes, such as TRACE/PARCS, to calculate three-dimensional thermal hydraulic and neutronic parameters for the entire core or to provide a basis for conservative evaluations of the hot-channel safety analysis applications (RETRAN).

7. References

1. U.S. NRC: TRACE V5.840 user's manual, U.S. NRC, 2014.
2. Paulsen, M. P.; McFadden, J. H.; Gose, G. C.; Peterson, C. E.; Jensen, P. J.; Shatford, J. G.; McClure, J. A.; Westacott, J. L.: RETRAN-3D—A Program for Transient Thermal Hydraulic Analysis of Complex Fluid Flow Systems. Computer Code Manual, NP-7450, Vol. 1, Revision 3, 1998.
3. Berna, G. A.; Beyer, C. E.;Davis, K. L.; Lanning, D. D.: FRAPCON-3:A Computer Code for the Calculation of Steady-State, Thermal- Mechanical Behavior of Oxide Fuel Rods for High Burnup. NUREG/CR-6534, Vol. 3, PNNL-11513, USA, 1997.
4. Yu- Ting Ku; Yung-Shin Tseng; Jong-Rong Wang; Chunkuan Shih; Y. M. Ferng: Thermal Hydraulic Behavior in Lower Plenum of Chinshan Nuclear Power Plant Using Computational Fluid Dynamics, 2013 ANS Winter Meeting, USA, 2013.
5. ANSYS: FLUENT V12 Theoretical Manual. ANSYS Inc., 2009.
6. ANSYS: FLUENT V12 User Defined Function Manual. ANSYS Inc., 2009.
7. Van Doormaal, J. P.; Raithby, G. D.: Enhancements of the SIMPLE Method for Predicting Incompressible Fluid Flows. Numerical Heat Transfer 7 (1984) 147-163, DOI:10.1080/01495728408961817.

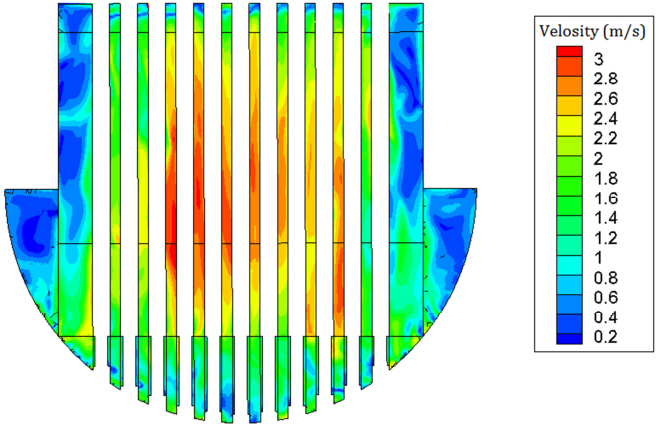

Fig. 12 Velocity distribution of lower-plenum.

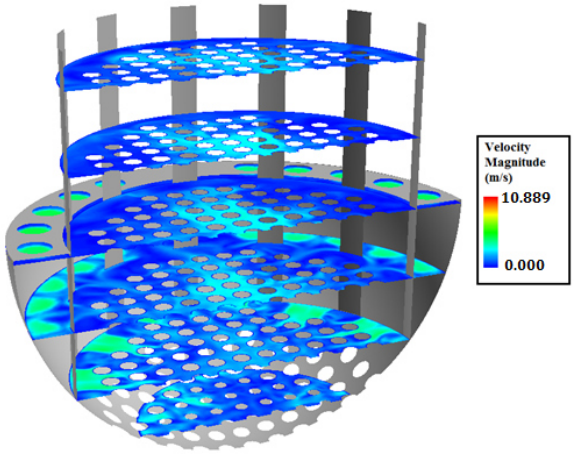

Fig. 13 Velocity distribution of different height in lower-plenum.

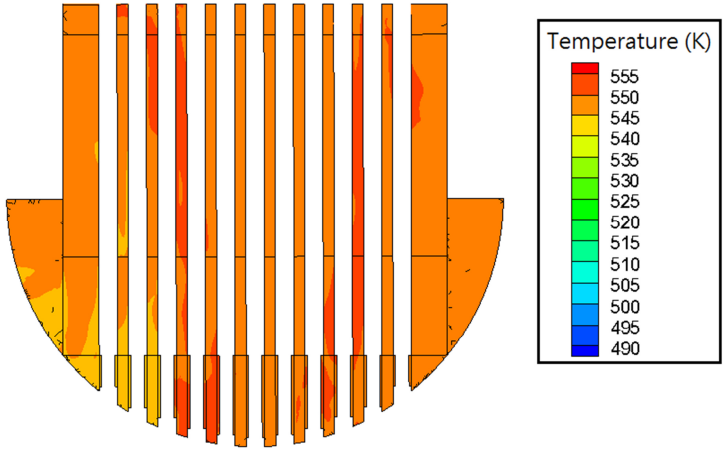

Fig. 14 Temperature distribution of lower-plenum.

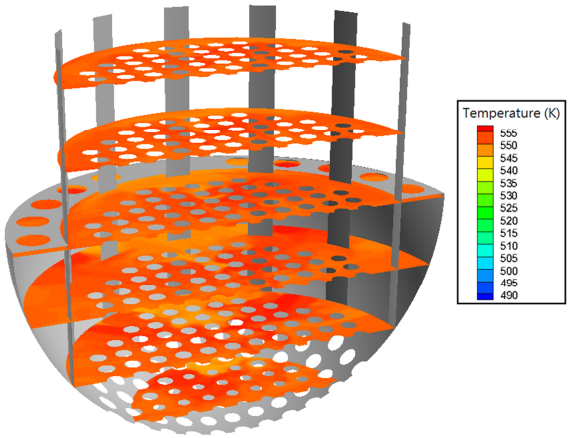

Fig. 15 Temperature distribution of different height in lower-plenum.